CHEMCONFLUX[20] Special Issue

J. Indian Chem. Soc.,
Vol. 97, No. 10a, October 2020, pp. 1678-1682

Methanol sensing using catalyst free nickel foam modified with solvo-thermally synthesized magnetite (Fe_3O_4) nanoparticles

Bhim Sen Yadav, Anand Kumar Vishwakarma and Naresh Kumar*

Department of Physics, Motilal Nehru National Institute of Technology Allahabad, Prayagraj-211 004, Uttar Pradesh, India

E-mail: nsisodia@mnnit.ac.in

Manuscript received online 16 July 2020, revised and accepted 31 October 2020

In the present study, methanol has been detected by studying variation in the area enclosed in the I-V curve of cyclic voltammograms. Nickel foam modified with magnetite (Fe_3O_4) nanoparticles prepared by solvo-thermal method was utilized as a working electrode. X-Ray diffraction analysis has been accomplished for the prepared working electrode and it affirms the pure polycrystalline phase of Fe_3O_4 along with nickel peaks. Magnetic measurements (M-H curve) for nanoparticles of Fe_3O_4 records the value of saturation magnetization to be 53 emu/g. Cyclic voltammetric study for prepared electrode has been used to detect methanol present in an electrolyte solution. Corresponding results reveal that the addition of 100 μM of methanol in an alkaline electrolyte consisting of 1 *M* NaOH causes a substantial increment in the area enclosed in the I-V curve. Moreover, an increase in the value of the scan rate of voltage admits enhancement in area enclosed in I-V curve and peak currents as well. Results obtained can be used to develop a handheld biosensor for methanol.

Keywords: Magnetite, sensing, nanoparticles, cyclic voltammograms, Verwey transition.

Introduction

Magnetite (Fe_3O_4), as one of the oldest magnetic materials possess an inverse spinel crystal structure. Owing to unique magnetic properties like the highest known Curie temperature (860 K), 100% spin polarizability and good conductivity at room temperature among the ferrites, Fe_3O_4 has been studied extensively for possible candidates in spintronic devices. At low temperatures magnetite undergoes a first order transition, namely, Verwey transition (T_V), located at T_V ~115–125 K depending on sample conditions, whose physical nature has not yet been fully understood[1]. Due to facile synthesis options, biocompatibility, and remarkable catalytic activity of Fe_3O_4, nowadays, it became a rising choice for biosensing applications[2]. In recent years, electrochemical biosensors based upon Fe_3O_4 nanoparticles have been explored extensively. A complete study of the amperometric determination of bisphenol-A (BPA) was reported by Yu *et al.* by using chitosan-Fe_3O_4 (CS-Fe_3O_4) nanocomposite modified glassy carbon electrodes and it was found that low detection limit, high sensitivity, improved stability, and repeatability were name to be a few outcomes[3]. Selective electrochemical sensing of arsenite in water has been accomplished by Devi *et al.* using a glassy carbon electrode modified with noble metal-free reduced graphene oxide-Fe_3O_4 nanocomposite via square wave anodic stripping voltammetry (SWASV)[4]. In their study, the enhanced electrochemical performance was reported with a sensitivity of 0.281 μA/ppb and a theoretical limit of detection of 0.12 ppb towards arsenite. Lately, Ni foam modified with Fe_3O_4 nanoparticles also came out to play an important role in electrochemical sensing of various pollutants due to the availability of large electroactive sites present in Fe_3O_4 nanoparticles entrapped within pores of Ni foam.

Methanol, also known as wood alcohol is very important as it is immeasurably utilized in various fields like in chemical synthesis, as clean burning-fuel, as automobile antifreeze, and in rendering ethyl alcohol unfit for drinking, and so on. Due to its uptake on a large scale, the toxicity of methanol has been explored for safety intentions and it was found to be a dangerous poison causing life-threatening diseases[5]. On account of its toxicity, methanol sensing has been delved into much depth and published in several studies. Most of

the studies included sensing mechanisms of methanol in its gaseous form[6]. In our study, methanol sensing was accomplished by performing cyclic voltammetric measurements using nickel foam modified with Fe_3O_4 nanoparticles as a working electrode.

Experimental

Materials:

The experiment has been performed with iron(III) chloride ($FeCl_3$) (98%) purchased from CDH and urea extra-pure crystals obtained from Merck. The solvent involved was prepared by mixing Rankem-made ethylene glycol ($C_2H_6O_2$) and ethanol (C_2H_5OH). Oleylamine micelles were utilized within the synthesis and bought from CDH. All the chemicals were used as received without any further purification.

Fabrication of electrode:

Synthesis involves the preparation of a precursor solution by adding a stoichiometric measure of Fe_3O_4 in solvent prepared by mixing ethanol and ethylene glycol. Urea and olyelamine have been included further with continuous stirring. Ni foam of known dimensions was added in solution and further treated solvothermally for 15 h in stainless steel autoclave. Subsequently, Ni foam coated with magnetite nanoparticles (Fe_3O_4/NF) was washed and dried further to be utilized as a working electrode (Fig. 1)[7].

Structural investigations were finished with an X-ray diffractometer (XRD) (Make: Rigaku, Model: Smart lab 3 kW) operated at 40 kV/30 mA with Cu-K_α radiation (1.5406 Å) followed by magnetic measurements using a Vibrating Sample Magnetometer (VSM) (Quantum Design, USA; Model: VersaLab, 3 Tesla). Electrochemical studies were performed by using a three-electrode system in Metrohm auto lab (PGSTAT 304 N) constituted of Fe_3O_4/NF as a working electrode, platinum rod as counter electrode and Ag/AgCl as a reference electrode in the electrolyte solution of 1 *M* NaOH (Fig. 2).

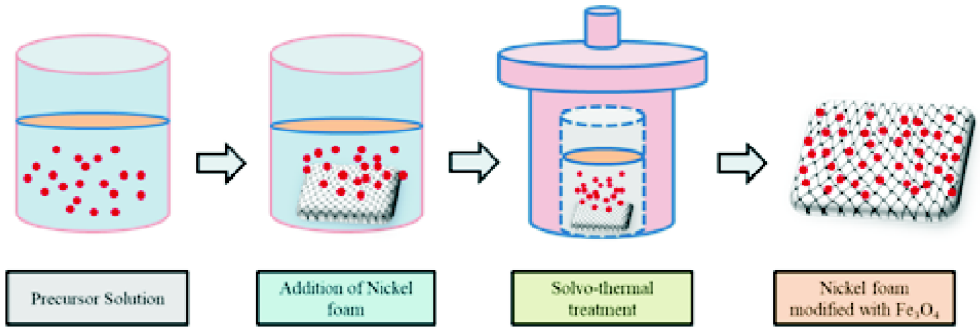

Fig. 1. Schematic diagram representing the synthesis process of Fe_3O_4/NF working electrode.

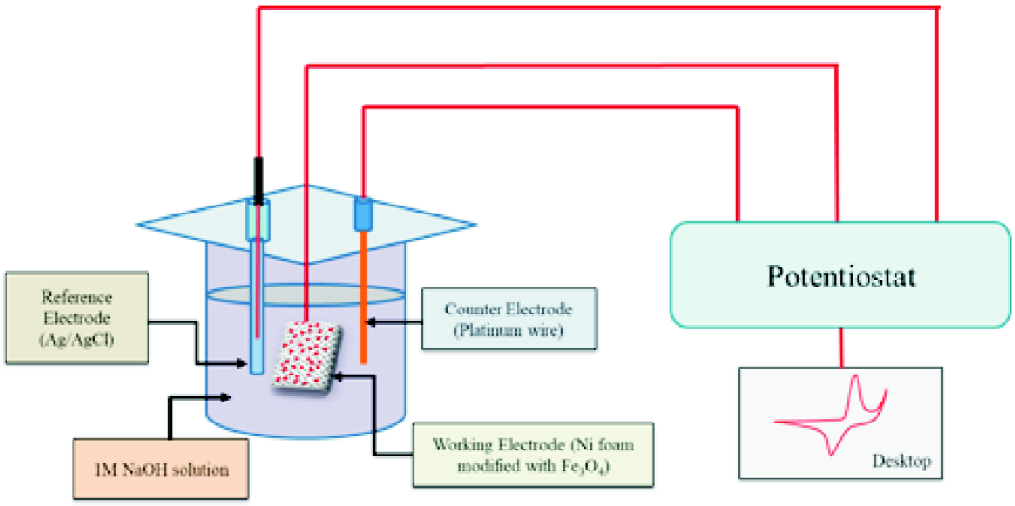

Fig. 2. Schematic representation of the three-electrode system.

Results and discussion

Structural analysis:

Structural characterization performed via an X-ray diffractometer proclaimed the formation of a single-phase nanocrystalline magnetite (Fe_3O_4). Fig. 3a shows the XRD plot associated with bare nickel foam and nickel foam modified with Fe_3O_4 nanoparticles. Also, an enlarged view of the XRD plot portraying clear sight of peaks belonging to Fe_3O_4 nanoparticles was shown in Fig. 3b. As seen in the graph 3a, characteristic peaks of Fe_3O_4 (marked as '#') were indexed at different 2θ values as (220), (311), (400), (511), and (440), respectively and belongs to space group Fd3m (JCPDS card no. 00-019-0629).

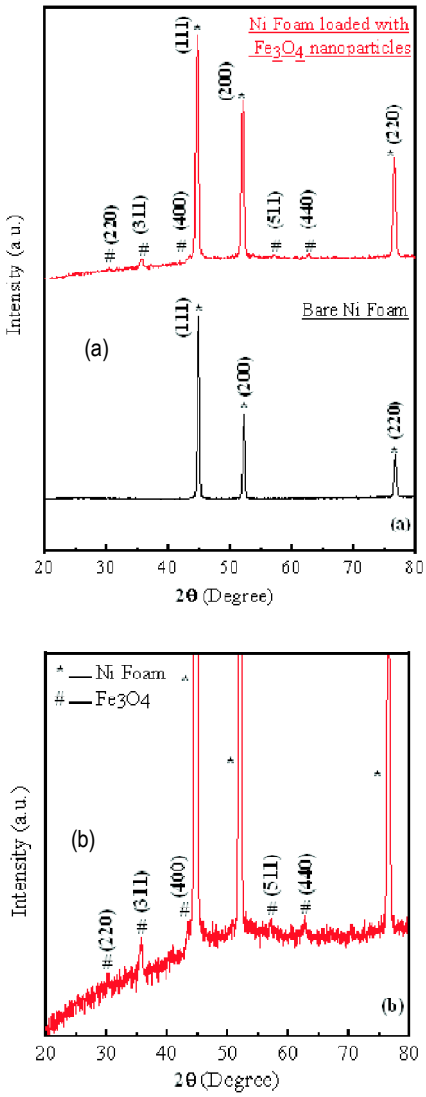

Fig. 3. (a) XRD plot for bare Ni foam and electrode consisting of Ni foam modified with magnetite nanoparticles, (b) enlarged view of XRD plot revealing peaks of Fe_3O_4.

Along with peaks of Fe_3O_4, there are other peaks indexed as (111), (200), and (220) at 2θ values (marked as '*') of 44.76°, 52.1° and 76.58°, respectively can also be observed with strong intensities and were assigned to Nickel foam substrate. The lattice parameter of Fe_3O_4 was also evaluated using 2θ values and noted to be 8.4056 Å, claiming the formation of a defect-free phase of magnetite with a balanced stoichiometric ratio of Fe:O and was in agreement with JCPDS card no. 00-019-0629[8].

Magnetic properties:

Magnetic properties for the prepared Fe_3O_4 nanoparticles were recorded at room temperature by employing Vibrating Sample Magnetometer (VSM) and plotted graph for magnetization vs the applied magnetic field (Oe) showed in Fig. 4a. The obtained M-H loop achieved the saturation magnetization (M_S) of 53 emu/g and a very low coercivity value of 85 Oe was also estimated (inset of Fig. 4a). The value of saturation magnetization 53 emu/g is much lower than that of bulk saturation magnetization value of 90 emu/g and may be due to the anisotropy in crystal, irregular arrangement of sublattices, or variation in particles size. Also, the existence of a magnetic dead layer around the surface of the nanoparticles contributes to a reduction in the saturation magnetization value[9,10].

To explore the magnetic behavior at low temperature, normalized magnetization viz. M(T)/M (50 K) vs temperature were scanned also and strikingly, rarest characteristic property, Verwey Transition (VT) for Fe_3O_4 was evidenced near 110 K (Fig. 4b). At Verwey transition temperature (T_V), a sudden increase in magnetization value was exhibited due to John-Teller distortion involving perturbed distortion of cubic spinel structure into the monoclinic structure by Fe^{3+} ions of octahedral sites in Fe_3O_4[11]. Depending upon variation in parameters of synthesis of Fe_3O_4 viz. temperature, cationic distributions, oxygen deficiency, etc. different values of T_V have been accounted for within the range of 120–180 K. In our case, VT appeared at a T_V value of 110 K due to one of the possible reasons.

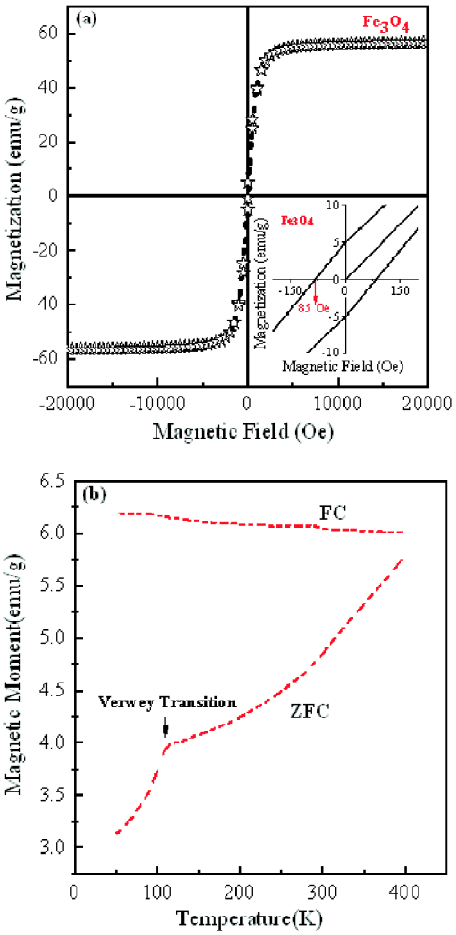

Fig. 4. (a) Magnetization vs magnetic field plot for Fe_3O_4 (with an inset picture depicting hysteresis loop and coercivity), (b) normalized magnetization vs temperature curve showing Verwey transition for Fe_3O_4.

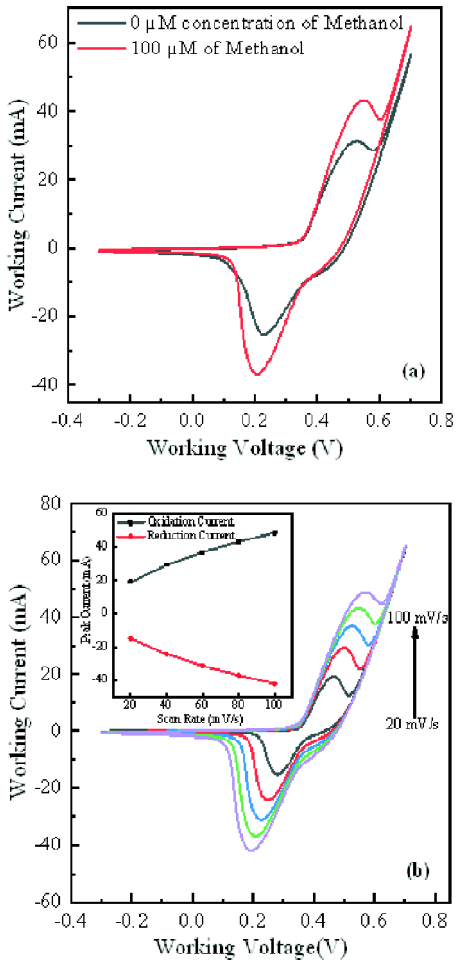

Fig. 5. (a) Cyclic voltammograms of Fe_3O_4/NF electrode with 0 μM and 100 μM concentrations of methanol, (b) magnetite modified nickel foam electrode at scan rate of 20, 40, 60, 80, and 100 mV/s; inset showing variation in peak current at different scan rates.

Electrochemical measurements:

Prepared Fe_3O_4/NF electrode was used for detection of 100 μM concentration of methanol in alkaline medium constituting of 1 *M* of NaOH solution via cyclic voltammetry (CV). Fig. 5a shows the CV curve of Fe_3O_4/NF performed in 1 *M* of NaOH solution with 0 μM and 100 μM concentration of methanol (CH_3OH) at a scan rate of 80 mV/s. The appearance of redox peaks in both cases was ascribed to the charge transfer process of solid-state redox. Upon the addition of methanol, the CV curve admitted approximately enhancement of ~38% in both oxidation and reduction current. A quite large enhancement in oxidation and reduction current appeared because Fe_3O_4 being a hub of large electro-active sites causes feasible electro-oxidation of methanol.

Here, Fe_3O_4 acted as a catalyst for electro-oxidation of methanol, and the mechanism during the process involves adsorption of reactants on the surface of Fe_3O_4 and then conversion in intermediated species, and lastly the formation of products[12,13]. Fig. 5b depicts CV investigation of Fe_3O_4/NF electrode as a function of scan rate from 20 mV/s to 100 mV/s with an interval of 20 mV/s and it can be estimated that magnitude of both reduction and oxidation current increases rapidly with scan rate (inset) signaling better improved catalytic behavior of electrode.

Conclusions

To summarize, working electrode Fe_3O_4/NF has been

successfully synthesized via the facile single-step solvothermal method and structural analysis declared synthesis of pure crystalline spinel phase of Fe_3O_4 on Ni foam substrate. The lattice parameter value was 8.4056 Å which exacted the formation of the defect-free phase of Fe_3O_4. The low value of saturation magnetization of 53 emu/g was recorded and departure from bulk value was explained on the basis of the presence of magnetically dead layer hindering exchange interaction among the surface of Fe_3O_4 nanoparticles and core spin. Methanol sensing is done via observing variation in redox currents of cyclic voltammograms which amazingly, acknowledged about ~38% enhancement in both oxidation and reduction current upon addition of 100 μM of methanol. Electro-oxidation of methanol was assigned as the reason for enhancement in current values and Fe_3O_4/NF was found to be acting as a catalyst in electro-oxidation. The present study demonstrated primary outcomes of methanol sensing and results are inevitably interesting for the fabrication of biosensors for methanol using Fe_3O_4/NF as a working electrode.

Acknowledgements

The authors acknowledge CIR, MNNIT Allahabad.

References

1. S. Singh, N. Kumar, A. Jha, M. Sahni, K.-d. Sung, J. H. Jung and S. Chaubey, *J. Mater. Sci.: Mater. Electron*, 2014, **26**, 32.
2. N. Sanaeifar, M. Rabiee, M. Abdolrahim, M. Tahriri, D. Vashaee and L. Tayebi, *Anal. Biochem.*, 2017, **519**, 19.
3. C. Yu, L. Gou, X. Zhou, N. Bao and H. Gu, *Electrochim. Acta*, 2011, **56**, 9056.
4. P. Devi, C. Sharma, P. Kumar, M. Kumar, B. K. S. Bansod, M. K. Nayak and M. L. Singla, *J. Hazard. Mater.*, 2017, **322**, 85.
5. N. Permpalung, W. Cheungpasitporn, D. Chongnarungsin and T. M. Hodgdon, *N. Am. J. Med. Sci.*, 2013, **5**, 623.
6. P. K. Kannan and R. Saraswathi, *Talanta*, 2014, **129**, 545.
7. M. Mandal Goswami, *Sci. Rep.*, 2016, **6**, 35721.
8. E. J. Fasiska, *Corros. Sci.*, 1967, **7**, 7.
9. S. Ayyappan, G. Panneerselvam, M. P. Antony, N. V. Rama Rao, N. Thirumurugan, A. Bharathi and J. Philip, *J. Appl. Phys.*, 2011, **109**, 084303.
10. A. Millan, A. Urtizberea, N. J. O. Silva, F. Palacio, V. S. Amaral, E. Snoeck and V. Serin, *J. Magn. Magn. Mater.*, 2007, **312**, L5.
11. M. Bohra, N. Agarwal and V. Singh, *J. Nanomater.*, 2019, **2019**, 1.
12. H. S. Jadhav, A. Roy, W.-J. Chung and J. G. Seo, *Electrochim. Acta*, 2017, **246**, 941.
13. G. M. Thorat, H. S. Jadhav and J. G. Seo, *Ceram. Int.*, 2017, **43**, 267.